

Abundance sensitive points of line profiles in the stellar spectra

V. A. Sheminova^{1*} and C. R. Cowley^{2†}

¹Main Astronomical Observatory, National Academy of Sciences of the Ukraine, 27 Akademika Zabolotnoho St., 03680 Kiev, Ukraine

²Department of Astronomy, University of Michigan, Ann Arbor, MI 48109-1042, USA

Accepted 2013 Month 00. Received 2013 Month 00; in original form 2013 Month 00

ABSTRACT

Many abundance studies are based on spectrum synthesis and χ -squared differences between the synthesized and an observed spectrum. Much of the spectra so compared depend only weakly on the elemental abundances. Logarithmic plots of line depths rather than relative flux make this more apparent. We present simulations that illustrate a simple method for finding regions of the spectrum most sensitive to abundance, and also some caveats for using such information. As expected, we find that weak features are the most sensitive. Equivalent widths of weak lines are ideal features, because of their sensitivity to abundances, and insensitivity to factors that broaden the line profiles. The wings of strong lines can also be useful, but it is essential that the broadening mechanisms be accurately known. The very weakest features, though sensitive to abundance, should be avoided or used with great caution because of uncertainty of continuum placement as well as numerical uncertainties associated with the subtraction of similar numbers.

Key words: line: profiles – Sun: abundances – Stars: abundances.

1 INTRODUCTION

Since the early days of analytical stellar spectroscopy, it has been known that equivalent widths have numerous advantages over the use of profiles. It is easily demonstrated that equivalent widths are unaffected by various and often uncertain broadening mechanisms, both stellar and instrumental (see below). Nevertheless, modern methods have made it possible to synthesize large regions of the spectra of many stars. Following the pioneering paper by Valenti & Piskunov (1996), *Spectroscopy Made Easy*, considerable work has been based on automated methods, some based on equivalent widths, but many stressing spectral synthesis (cf. Sbordone et al. 2014, Blanco-Cuaresma et al. 2014, and references therein). While these methods have been demonstrated to work quite well, they could be strengthened *by incorporating knowledge of wavelengths sensitive to the stellar properties sought*.

We emphasize abundances here. In practice other factors (T_e , $\log(g)$, microturbulence) must be known, and generally must be sought simultaneously with abundances. This is a strength of some of the automated methods. The basic technique we advocate could be adapted for these other parameters, but that is not done here.

For the most part, automated methods are used with cooler stars, where the abundance patterns are of limited scope, e.g. [Fe/H] or [α /Fe] variations. The situation is more subtle with chemically peculiar stars (CP) of the upper main sequence, or peculiar red giants, where element-to-element variations can be large. The analysis of young stars are also problematical, where standard, LTE models are of questionable validity, especially in the region where the cores of strong lines are formed.

Our goal is to show that knowledge of abundance-sensitive regions of line profiles make it possible to improve accuracy. We illustrate how inaccuracies can arise from the use of regions of line profiles less sensitive to abundance than other factors such as turbulence, or damping.

2 SENSITIVITY OF THE PROFILE POINTS TO ABUNDANCE

It is convenient to consider changes in line profiles resulting from abundance variations one element at a time. In the present examples the element will be iron. We use the symbol $A = 12 + \log(\text{Fe}/N_{\text{tot}})$ for abundances on the usual logarithmic scale, where for hydrogen $A = 12.00$, Fe/N_{tot} is the number of iron atoms and ions to the sum for all elements including iron. The illustrations are all simulations where the input parameters are precisely known. We vary abun-

* E-mail:shem@mao.kiev.ua (VAS)

† E-mail:cowley@umich.edu (CRC)

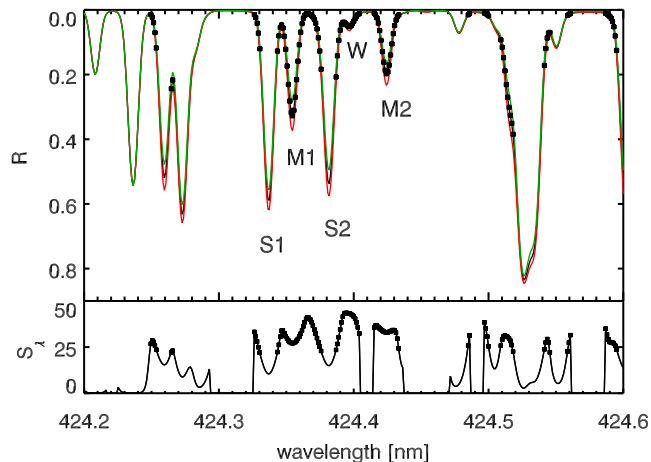


Figure 1. Line depth $R_\lambda = (F_c - F_\lambda)/F_c$ calculated with assumed iron abundance $A = 7.46$ (black), $A - 0.1$ (green), $A + 0.1$ (red). The sensitivity function S_λ is shown in the subfigure, with the most sensitive points indicated. Only the iron abundance has been changed. Here, and in the following figures, colors refer to the online version.

dance, microturbulence (ξ_t), rotation ($V \cdot \sin(i)$), and the macroturbulence (V_{mac}). The latter is taken to be a Gaussian, and assumed here to include instrumental broadening. In most stellar work, the macroturbulence is assumed to be isotropic with a Gaussian profile. Gaussians are also typically assumed for instrumental profiles.

Let the parameter defining the profile of an absorption line be the line depth, $R_\lambda = (F_c - F_\lambda)/F_c$. Here F_λ and F_c are the flux at the wavelength λ in the line profile and continuum, respectively. Following Cowley (1995) the sensitivity of each profile point to the A -variations may be calculated by the ratio

$$S_\lambda = 100 \cdot \frac{R_\lambda(A + \Delta A) - R_\lambda(A - \Delta A)}{R_\lambda(A)}.$$

The spectra are calculated with an assumed abundance A and again with A varied by $\pm \Delta A$. We adopted $\Delta A = 0.1$ dex to avoid large changes in the line profiles. Essentially the same information is obtained with other small values of ΔA . In this way we can calculate the sensitivity of each point of line profile to abundance without involving the more complex response functions which involve partial derivatives of the emergent flux with respect to the free parameters (see, e.g., Beckers & Milkey 1975; Caccin et al. 1977; Sheminova 1993).

Calculations are based on the synthesis code SPANSAT (Gadun & Sheminova 1988), and a MARCS model atmosphere (Gustafsson et al. 2008) with $T_{\text{eff}} = 5777$ K, $\log(g) = 4.44$, and the chemical composition of the Sun (Asplund et al. 2009). Local thermodynamic equilibrium (LTE) is assumed throughout. The MARCS model is available online at <http://marcs.astro.uu.se>. We use a depth-independent microturbulence $\xi_t = 1 \text{ km s}^{-1}$, corresponding to that used in the MARCS model and an isotropic macroturbulence of 2.4 km s^{-1} . The rotational velocity ($V \cdot \sin(i) = 1.85 \text{ km s}^{-1}$ (Bruning 1984)) was simulated by direct averaging over the disk. The synthesis of spectral regions includes the full list of lines available in the VALD database (Kupka et al. 1999), with line parameters: wavelengths, ex-

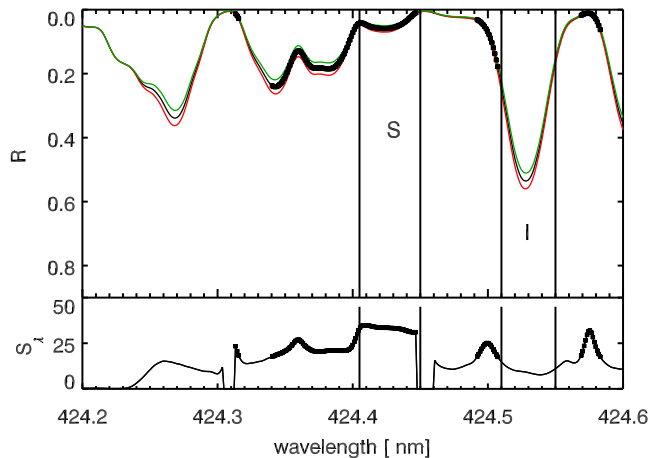


Figure 2. The same as Fig. 1 but with relatively high rotation velocity $V \sin i = 15 \text{ km s}^{-1}$. Symbols ‘S’ and ‘I’ mark regions sensitive and insensitive to the iron abundance.

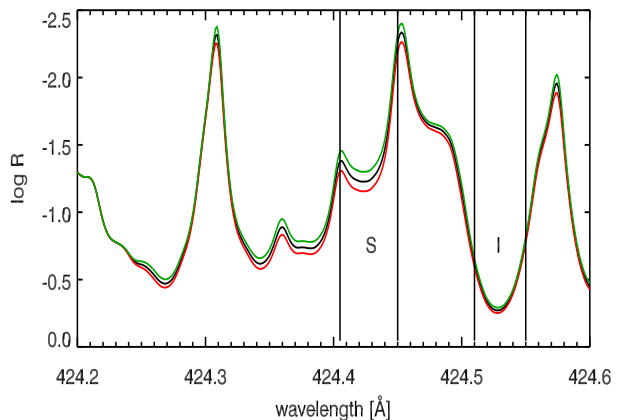


Figure 3. This plot was made with different parameters from those of Fig. 2. The logarithmic display makes the sensitivity of weak features more obvious than traditional plots of rectified spectra and fitted calculations.

citation potentials, oscillator strengths, and damping parameters.

A few features that are in the real solar spectrum are not in our calculation. These include molecular lines, not in our version of VALD, as well as unidentified or unclassified atomic lines.

2.1 High resolution and narrow-lined spectrum

The eye is drawn most naturally to the cores of the stronger lines, where the separation for the different abundances is most evident. The calculated sensitivity function shows how deceptive this visual impression can be. The cores of the stronger features are generally the *least* sensitive parts of the profile to abundance.

The most sensitive feature in Fig. 1 is the weak absorption at 424.395 (W), which shows the advantage of using weak lines for abundances. The two stronger lines, S₁ and S₂ are sensitive only in their wings. The moderately strength lines, M₁ and M₂ show intermediate cases. While the wings of moderate and strong lines can also be quite sen-

sitive to abundances, these regions are also sensitive to other, sometimes quite complicating factors. Beyond the Doppler core, the wing strength depends on the product of the abundance, the line strength, and the damping constant. Hyperfine structure, and Zeeman broadening could be relevant. In addition, the instrumental profile must be accurately known as well as broadening due to stellar turbulence (micro and macro), before accurate abundances can be determined from line wings.

These factors have virtually precluded the practical use of line wings in most abundance studies. There is, however, new work in which advantage could be taken of the sensitivity of line wings. We refer specifically to the new differential work on abundances of solar-type stars (e.g. Meléndez et al. 2009; Meléndez 2013). Thus far, this work has been based on equivalent widths. However, in comparing two closely similar stars, with spectra obtained by identical instruments, and reduced with the same procedures, the unknown broadening mechanisms should cancel. There is thus good reason to hope that these differential methods can be strengthened through the use of line wings.

2.2 Lower resolution and convoluted profiles

A great deal of important work deals with convoluted spectra, where it may not be possible to analyze weak, isolated features. This convolution may arise from the use of low instrumental resolution or in studies of integrated spectra of stellar systems. Sensitivity functions should be comparably useful in all of these cases. The spectra of single stars are often convoluted by rotation, which we discuss here.

The region shown in Fig. 2 is the same as in 1 but the profiles were broadened by an assumed rotation. The appearance of the spectra and the sensitivity functions themselves are markedly changed. Wider regions of the spectrum are now sensitive, though the sensitivities themselves are lowered – in the case of the maxima, by some 21 per cent. It would surely be useful for an abundance worker to see that the region from 424.41 to 424.45 nm was relatively sensitive (S) to the iron abundance while that from 424.51 to 424.55 was not (I).

2.3 Logarithmic plots

Traditional plots showing observed and calculated spectra obscure the sensitivity of weak features that is shown by the sensitivity functions. A 20 % change of a feature that is only 10 % deep makes a change in the depth of only 0.02 in the depth. This difference is hardly noticeable on a standard plot. By contrast, a change of only 5% on a line of depth 0.9 makes a change of 0.045, more than double the much larger *percentage* change of the weaker feature.

It might be helpful for abundance workers to use plots in which the logarithms of line depths are plotted rather than linear, relative fluxes. An example is shown in the Fig. 3, it conveys much the same information as the lower part of Fig. 2. The logarithmic plot compresses the larger line depths; the (online color) separation in the sensitive regions are more obvious while that for the stronger cores are suppressed. A logarithmic plot similar to Fig. 3, but showing observed and calculated spectra would help to focus attention on the weaker, more abundance-sensitive parts of the

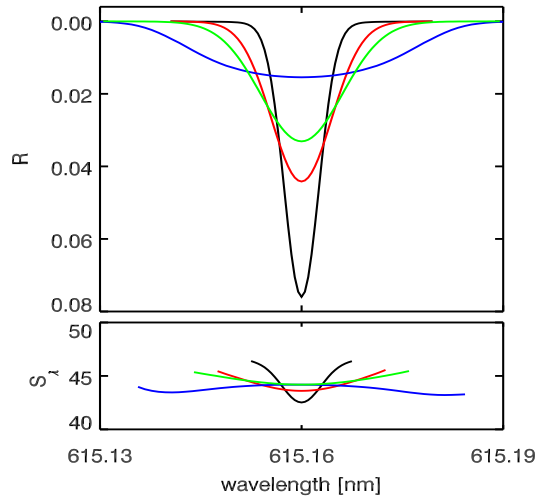


Figure 4. These four profiles all have the same equivalent width, and were made with the same abundance. Only the broadening parameters differ (see Tab. 1). Lower panel shows the sensitive functions of these profiles in their respective colors.

Table 1. Parameters used for the four profiles of Fig. 4. The listing is from the narrowest to broadest profile.

Pro.	A log	ξ_t km s ⁻¹	V_{mac} mÅ	$V \cdot \sin(i)$ km s ⁻¹	W mÅ
1	7.46	1.0	0.6	0.0	4.96
2	7.46	1.4	2.4	0.0	5.00
3	7.46	2.0	3.4	0.0	5.05
4	7.46	1.4	2.4	10.0	5.01

spectra. Unlike the sensitivity functions, such plots do not have the ability to display sensitivity to specific elements.

3 WEAK FEATURES

In this section a number of calculations are presented, based on the Fe I line at 6151.62 Å. Its (lower) excitation potential is 2.18 eV. The $\log(gf)$ given by Wiese & Fuhr (2006) is -3.29 . However, this value is varied for purposes of illustration. All profiles described in this section were calculated with the wavelength step of 5 mÅ and MARCS solar model.

3.1 Equivalent widths and profiles

The independence of equivalent widths of weak lines is illustrated in Fig. 4, where very different profiles yield the same abundances. This of course is a well known result. We use it here to emphasize that in this case, all of the relevant points are sensitive in the sense used in this paper. The sensitive function of each profile is high although it varies slightly with line depth. The parameters used in Fig. 4 are given in Table 1.

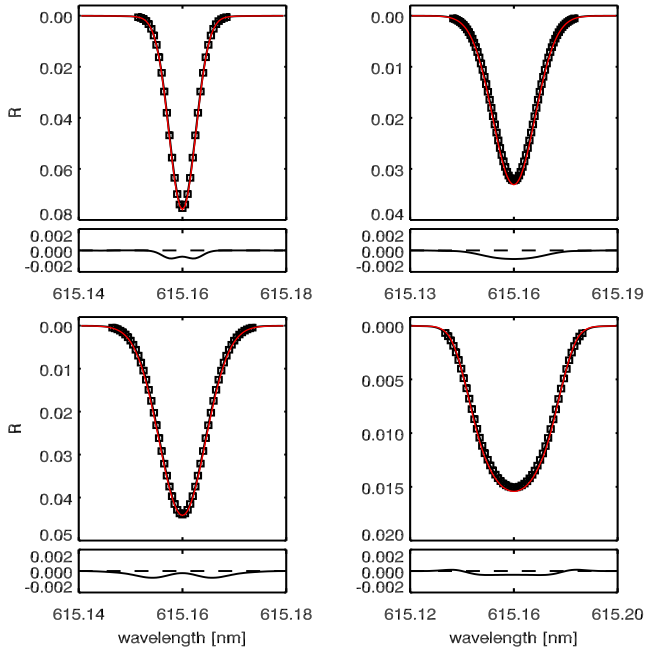


Figure 5. The red profiles are the same as in Fig. 4. The squares refer to calculations made with the abundances, $\log(gf)$ and ξ_t frozen at 7.46, -4.65, and 0.4, respectively, but with V_{mac} adjusted to obtain an acceptable fit. Residuals ($\Delta R = R - R_{\text{original}}$) are shown in the lower panels of each subfigure.

3.2 Weak-line fits with variable parameters

A numerical experiment shows that a close fit to the line profiles does not necessarily fix the microturbulence uniquely. Alternately, one may say that one can get a good abundance from weak lines, even if the microturbulence is not accurately known. In Fig. 5 we match individually, the four profiles of Fig. 4 with altered parameters. The four profiles of Fig. 4 are all closely matched with the abundance (7.46), $\log(gf)$ (-4.65), microturbulence (0.4 km s^{-1}), and $V \cdot \sin(i)$ as in Table 1. But V_{mac} was adjusted to obtain optimum fits. For Profiles 1-4, the best-fitting values of V_{mac} were 1.1, 2.7, 3.9, and 3.0 km s^{-1} .

3.3 Moderately weak lines

A similar experiment was performed for slightly larger equivalent widths. We froze the abundance (7.46), V_{mac} (2.4 km s^{-1}), and $V \cdot \sin(i)$ (0.0 km s^{-1}), and calculated equivalent widths and profiles for $\log(gf) = -4.30, -4.10$, and -3.96 . The corresponding equivalent widths were 10.5, 15.5, and $20.3 \text{ m}\text{\AA}$. We then tried to match these profiles by varying the abundances and V_{mac} . Relevant parameters for the fitted profiles are shown in Table 2. The corresponding figures are not shown as they closely resemble the fits of Fig. 5.

As we can see from Table 2, the accuracy of the abundance (determined by the difference $A_{\text{original}} - A_{\text{fit}}$) decreases with the increase of the equivalent width of the moderately weak lines. The uncertainties of the microturbulence can cause an error about 0.02–0.05 dex in the abundance derived from the profile fit of weak line with equivalent width of 10–20 $\text{m}\text{\AA}$. This is well within the typical accuracy of the oscillator strengths.

Table 2. Parameters of the best weak ($<21 \text{ m}\text{\AA}$) profile fits discussed in Section 3.3. Equivalent widths of the fitted profiles (W_{fit}) are the same (to $0.1 \text{ m}\text{\AA}$) as those of the original calculation (with $A_{\text{original}} = 7.46$) apart from Profile 3.

Pro.	W_{fit} $\text{m}\text{\AA}$	$\log(gf)$	ξ_t km s^{-1}	A_{fit}	V_{mac} km s^{-1}	χ^2/n
1	5.0	-4.65	0.4	7.46	2.7	$1.7 \cdot 10^{-7}$
2	10.5	-4.30	0.4	7.48	2.8	$3.4 \cdot 10^{-7}$
3	15.7	-4.10	0.4	7.50	2.8	$1.7 \cdot 10^{-7}$
4	20.3	-3.96	0.4	7.51	2.8	$4.0 \cdot 10^{-7}$

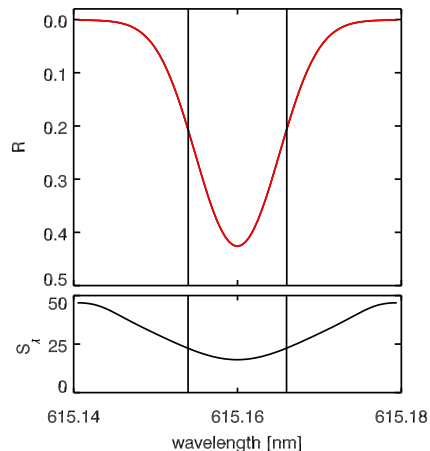


Figure 6. Sensitivity (black) and line depth profile (red) of calculated $53.4 \text{ m}\text{\AA}$ line in the solar flux. Note that the most sensitive parts of the profile to abundance lie where the line is very weak, or in a steep part of the profile. Vertical lines indicate the sensitivity level of 50% of the maximum S_λ shown.

4 INTERMEDIATE-STRENGTH LINES

It is our opinion that abundances should be based on weak lines ($W_\lambda \leq \approx 20 \text{ m}\text{\AA}$), whenever reliable oscillator strengths are available for them. In this and the next section we turn to a consideration of intermediate-strength, and strong lines, and illustrate their shortcomings. However, it would be a mistake to conclude that there is no abundance information

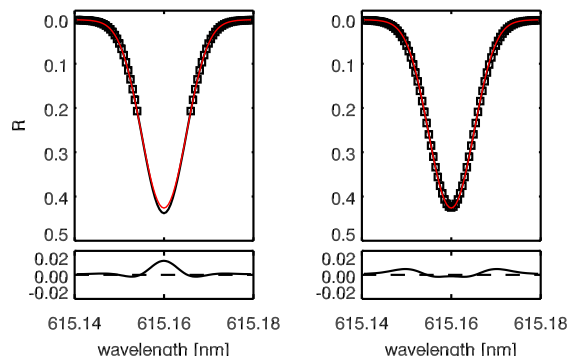


Figure 7. A best fit to the original (red) profile may be made for sensitive points (left, squares) with $\xi_t = 0.4$, $V_{\text{mac}} = 2.7 \text{ km s}^{-1}$, $A = 7.74$, $\chi^2/n = 8.8 \cdot 10^{-7}$ as well as for whole profile (right, with $\xi_t = 0.4$, $V_{\text{mac}} = 2.8 \text{ km s}^{-1}$, $A = 7.72$, $\chi^2/n = 4.8 \cdot 10^{-6}$).

Table 3. Parameters for Figs. 8, 9, and 10. $\log(gf)$ and $V \cdot \sin(i)$ are 0.00 for all three profiles. E_6 is an enhancement factor to the collisional damping.

Pro.	W mÅ	ξ_t km s ⁻¹	A	V_{mac} km s ⁻¹	E_6	χ^2/n
1	642.3	1.4	7.46	2.4	1.00	
2	636.5	1.4	7.24	2.4	1.75	$1.8 \cdot 10^{-8}$
3	692.4	3.4	7.46	2.4	1.00	$3.2 \cdot 10^{-7}$

in such features. In spite of their shortcomings it is sometimes necessary to work with them.

Curves of growth tell us that intermediate-strength lines are more sensitive to broadening mechanisms than abundance. For such features, a knowledge of sensitive points is not a great advantage. Apart from the risky regions with very small line depth, the more sensitive points lie in the steepest parts of the line profiles, where accurate measurements are difficult. Numerical experiments show that an underestimated microturbulence can be compensated by adjustments to the abundance and V_{mac} in such a way as to reproduce the original profile to an entirely acceptable accuracy. Yet the abundance difference could be more than 0.2 dex different from the correct value. This is illustrated in Figs. 6, and 7.

Figure 6 shows the sensitivity function and line-depth profile for a 53.4 mÅ line calculated in the solar flux with MARCS model. The following parameters were used in the calculation: $A = 7.46$, $\log(gf) = -3.29$, $\xi_t = 1.4 \text{ km s}^{-1}$, $V \sin i = 0$. The profile was convolved with $V_{\text{mac}} = 2.4 \text{ km s}^{-1}$.

In the numerical experiment, we set ξ_t to 0.4 km s^{-1} , and attempted to reproduce the original profile by adjusting the abundance and V_{mac} . Fig. 7 shows the best fit for the sensitive points is excellent ($A = 7.74$, $\chi^2/n = 8.8 \cdot 10^{-7}$), while for whole profile is fair ($A = 7.72$, $\chi^2/n = 4.8 \cdot 10^{-6}$), but should satisfy an abundance worker with a realistic sense of the uncertainties of this work. Note that the ‘new’ abundance is greater by 0.26–0.28 dex than the value originally assumed.

5 STRONG LINES

The wings of strong lines are potentially useful for abundances subject to the severe qualification that the broadening mechanisms be accurately known. The wing strength of a line depends directly on the product of the abundance, the oscillator strength, and the damping constant. Thus, the damping constant must be as accurately known as the oscillator strength. We illustrate this in Figs. 8, and 9, which are similar to the figures of Section 4.

We used the same Fe I line as Section 4, but changed the $\log(gf)$ from -3.29 to 0.00 and the wavelength step from 5 to 10 mÅ. With $A = 7.46$, $\xi_t = 1.4 \text{ km s}^{-1}$, $V_{\text{mac}} = 2.4 \text{ km s}^{-1}$, we obtain the 642.3 mÅ line shown in Fig. 8. For this line 75% of the maximum sensitivity shown corresponds $R = 0.18$. We can use the sensitive points in the wing regions of $0.02 < R < 0.18$ that are in a more gradually-sloping part of the profile than was the case for Fig. 7.

To demonstrate the degeneracy of abundance and

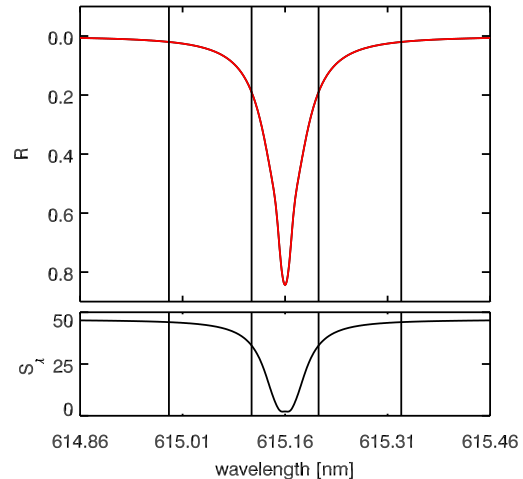


Figure 8. Sensitivity function (black) and depth profile (red) of a 642.3 mÅ line. The strips on either side of the line center show regions of the sensitive points, that was chosen with the sensitivity is greater than 75% of its maximum value (Table 3, Pro. 1).

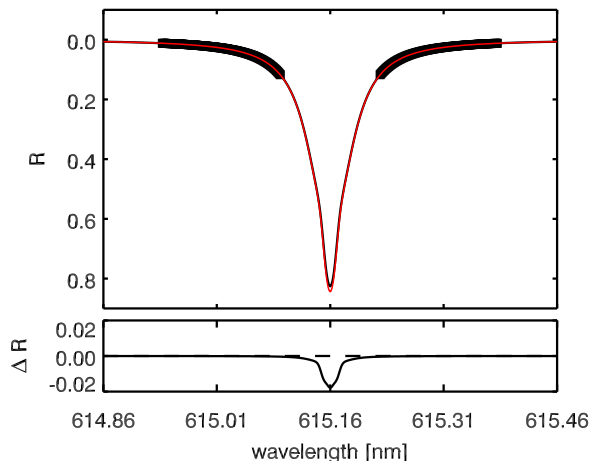


Figure 9. A best fit to the original (red) profile of a strong line may be made for sensitive points (black squares) with $E_6 = 1.75$, $A = 7.24$, $\chi^2/n = 1.8 \cdot 10^{-8}$ (Table 3, Pro. 2).

damping, we set the damping constant (C_6) increased by a factor $E_6 = 1.75$ and tried to compensate that by changing abundance. To get the best fit for this new line profile, the abundance *can* be determined from the wings of strong lines when the damping constants are accurately known. If rotation and macro-turbulence are significant, these factors must also be known.

In differential abundance work the often uncertain damping constants and oscillator strengths may largely cancel. The degree to which these factors could be important depends on how closely the differenced stars resemble one another. Residual effects of rotation or macro-turbulence must be carefully considered.

We now show (Fig. 10) the case of a strong line where the core is not well fit, but an excellent abundance would be obtained from a fit to the sensitive points. The sensitive region contains 313 points. The best fit to the sensitive points

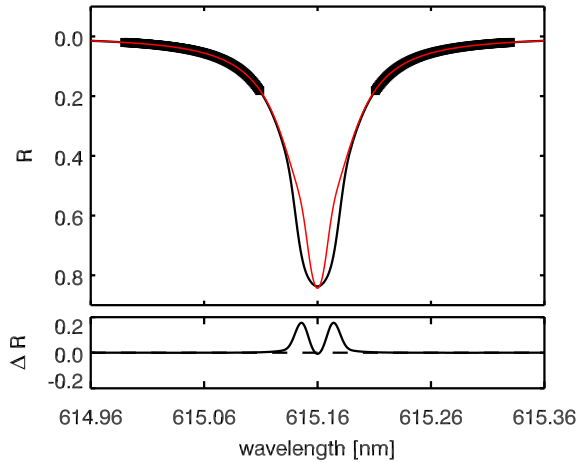


Figure 10. This strong line calculation (black) uses all parameters including the abundance and damping the same as the (red, Table 3, Pro. 1) calculation, but the microturbulence has been changed from 1.4 to 3.4 km s^{-1} (Table 3, Pro. 3).

gives the original $A = 7.46$ and a small χ^2/n of $3.2 \cdot 10^{-7}$. If the central region of the profile is included, there are 799 points, and the fit is obviously less good; $\chi^2/n = 7.2 \cdot 10^{-4}$.

In this section we have demonstrated that a fit to a strong line—including sensitive points—does not necessarily mean that a correct abundance will be obtained. On the other hand we show that even if the core of a strong line is poorly fit, an accurate abundance can be obtained when the broadening is accurately known.

6 SUMMARY

Not all portions of a stellar spectrum are equally sensitive to abundances. In this paper we showed that a good abundance not only depends on the choice of accurate atomic parameters, but the selection of features that are sensitive to abundances. We proposed a scheme to find abundance-sensitive regions. By far, the most useful features for abundances are weak lines with reliable gf -values. The use of weak features requires accurate continuum adjustment, which is rarely as accurate as 0.5 per cent. Unidentified blends or blends with inaccurate atomic parameters in the line wings do not allow the use of most profiles in the abundance analysis. However, we can select sensitive points in the profile parts are free from the blends or omit some points near the continuum where these effects are significant.

We show that moderately strong lines, in spite of having sensitive regions, are usually less good for abundance work due to their high sensitivity to turbulence. Today, the application of 1D atmosphere models and classical concepts of micro and macroturbulence are widely used and the problem of uncertainty of the synthetic profiles due to the micro and macroturbulence remains for sensitive profile points. While the line profile results obtained with 3D hydrodynamical (HD) stellar atmosphere models without any need for micro or macroturbulence are not without problems. Theoretical profiles of the moderate lines computed in 3D HD systematically underestimate the line width and that some

additional work on improving the atmospheric velocity field is still required (Scott et al. 2014).

Strong lines can be useful, especially in differential abundance work. The wings of very strong lines are insensitive to turbulence parameters and the NLTE-effects. They can be used for profile fits when the damping constants are well known.

We propose to using the sensitive points but recognize that other regions of the spectrum still contain abundance information.

Acknowledgements

We thank an unknown referee for patience, and suggestions to improve the paper.

REFERENCES

- Asplund, M., Grevesse, N., Sauval, A. J., & Scott, P. 2009, *ARA&A*, 47, 481
- Beckers J. M., Milkey R. W., 1975, *Sol. Phys.*, 43, 289
- Blanco-Cuaresma S., Soubiran C., Jofré P., Heiter U., 2014, *ASI Conf. ser.* 2014, Vol. 10, p. 1, ed. H. P. Singh & Ph. Prugniel
- Bruning D. H., 1984, *ApJ*, 281, 830
- Caccin B., Gomez M. T., Marmolino C., Severino G., 1977, *A&A*, 54, 227
- Cowley C. R., 1995, in Sauval A. J., Blomme R., Grevesse N., eds, *Laboratory and Astronomical High Resolution Spectra Vol. 81 of Astronomical Society of the Pacific Conference Series, Line and Element Identifications in CP Stars: History, Techniques, Results, and Prospectus*. p. 467
- Gadun A. S., Sheminova V. A., 1988, in Preprint of the Institute for Theoretical Physics of Academy of Sciences of USSR, ITF-88-87P, Kiev SPANSAT: the Program for LTE Calculations of Absorption Line Profiles in Stellar Atmospheres, pp 3–37
- Gustafsson B., Edvardsson B., Eriksson K., Jørgensen U. G., Nordlund Å., Plez B., 2008, *A&A*, 486, 951
- Kupka F., Piskunov N., Ryabchikova T. A., Stempels H. C., Weiss W. W., 1999, *A&A Suppl.*, 138, 119
- Meléndez J., 2013, arXiv:1307.5274
- Meléndez J., Asplund M., Gustafsson B., Yong D., 2009, *ApJ*, 704, L66
- Sbordone L., Caffau E., Bonifacio P. and Duffau S., 2014, *A&A*, 564, A109
- Scott P., Asplund M., Grevesse N., Bergemann M., and Sauval A. J., 2014, arXiv:1405.0287
- Sheminova V. A., 1993, *Kinematika i Fizika Nebesnykh Tel*, 9, 27
- Valenti J. A., Piskunov N., 1996, in *Model Atmospheres and Spectrum Synthesis*, ASP Conf. Ser. Vol. 108, ed. S. J. Adelman, F. Kupka, and W. W. Weiss, p. 175
- Wiese W. L. and Fuhr J. R., 2006, in Weck P. F., Kwong V. H. S., and Salama F., eds, *Proceedings of the NASA LAW 2006, New Critical Compilations of Atomic Transition Probabilities for Neutral and Singly Ionized Carbon, Nitrogen, and Iron*, p. 278